Robust Solution Approach for Bilevel Demand Response Game at Distribution Level

Yang Chen, Kadir Amasyali, Mohammed Olama, and Byungkwon Park

***Abstract*—In this paper, a bilevel electricity pricing and demand response game between a distribution system operator (DSO) and load aggregators (LAs) is considered, and a robust decision model is proposed for the DSO to deal with the uncertainties from the wholesale market prices and demand consumptions of LAs. With the max-min objective at the upper level, the robust bilevel model is converted into a single level model by the Karush-Kuhn-Tucker (KKT) conditions and prime-dual transformation. Several groups of experiments have been conducted based on different preferences on uncertainty gaps and peak load reductions to show its effectiveness. After-the-fact scenario analysis has indicated that the robust solution is more beneficial in reducing the risk of inaccurate predictions as compared to the risk neutral strategy.**

***Index Terms*—Stackelberg game, Demand response, Robust solution, Dual transformation, Load aggregator.**

NOMENCLATURE

Indices

T, t, n	Total hours, index for hours, LAs

Parameters

$C_t, \overline{P}$	Marginal cost, price upperbound
$\underline{H}_{n,t}, \overline{H}_{n,t}$	Lower & upperbound of thermal demand
$\underline{L}_{n,t}, \overline{L}_{n,t}$	Lower & upperbound of non-thermal demand
$Dh_{n,t}, Dd_{n,t}$	Nominal thermal, non-thermal demand
$\alpha_{n,t}, \theta$	Satisfaction preferences of LAs, penalty coef.
BI, ϵ	Initial level, Dissipation rate of virtual battery
$\underline{B}_{n,t}, \overline{B}_{n,t}$	Lowerbound, upperbound for virtual battery

Variables

$p_t, dl_{n,t}$	Electricity price, total electricity load
$hr_{n,t}, dr_{n,t}$	Resulted thermal load, non-thermal load
$m, b_{n,t}$	Peak load, storage level in virtual battery

I. INTRODUCTION

With the profound transformation of smart grids, new challenges arise for DSOs to manage the network in a safe and cost efficient manner. The flexibility of demand side management has offered an increasingly important and valuable resource to maintain system stability in an interactive and decentralized electricity grid [1]. In the United States, the combined wholesale demand response (DR) capacity of all regional system operators grew to 27 GW (around 6% of peak demand) in 2018, with an additional 5 GW offered through retail programs. Progress was particularly strong in California, where the capacity under auction doubled to 373 MW. Load control, interruptible services, and reserve markets also expanded elsewhere in the country [2].

Extensive research has been conducted to model the operational flexibility of DR at different levels, including a large body of studies in modeling the negotiation interaction between DSOs and LAs at the distribution level. In the negotiation game, the upper level DSO is generally set to have the privilege of setting the electricity price, while the lower level entities respond to the price and settle down the optimal demand. For instance, a Nash-bargaining based cooperative model is formulated for the DSO and LAs [3]; a tri-level DR model is developed for a grid operator, multiple service providers, and the corresponding customers [4]; a bilevel framework is also adopted for such pricing-demand negotiation [5] [6]; and a reinforcement learning algorithm is designed to obtain an optimal incentive strategy under incomplete information scenario in an edge-cloud framework [7]. In addition, to deal with uncertainties from renewables and demand, several scenario-based stochastic bilevel programming models are developed. In [8], a two-stage stochastic bilevel model is formulated, where an upper level system operator minimizes the total operation cost, and lower level LAs determine the DR trading shares through three DR options: load curtailment, load shifting, and load recovery. With the uncertainties from the market price and demand, a risk-constrained scenario-based stochastic bilevel framework is presented [9], where the upper level represents decisions from LAs, and the lower level models the customers' behaviors. The risk-aversion attitude of LAs is modeled using the conditional value at risk method.

In the authors' previous works [10] [11], deterministic and scenario-based stochastic bilevel models have been proposed for a DR game between a DSO and LAs with the consideration of the building customers' temperature preferences. However, the prediction error and risk attitude of the DSO were not considered. In this work, a robust decision approach is adopted to model the risk-aversion attitude of a DSO towards uncertainties on the electricity market price and

Y. Chen is with the Environmental Sciences Division, Oak Ridge National Laboratory, Oak Ridge, USA (email: cheny2@ornl.gov)

K. Amasyali, M. Olama, and B. Park are with the Computational Sciences and Engineering Division, Oak Ridge National Laboratory, Oak Ridge, USA (email: amasyalik@ornl.gov, olamahussemm@ornl.gov, parkb@ornl.gov)

demand profiles from LAs. In the upper level, the objective of the DSO is in max-min form to maximize the minimum payoff, while the LAs at the lower level maximize their own utility values.

II. Pricing-demand Response

In the investigated DR game here, the DSO is the leader that makes decisions on the electricity price by taking into account the demand responses from the LAs, which are followers in the lower level. The objective of the DSO is to maximize its overall utility, which includes its profit (first two terms in Eq.(1)), peak load penalty (fourth term in Eq.(1)), and the overall customer satisfaction (third term in Eq.(1)) that represents its social obligation.

$$\begin{aligned} DSO: \max U_o = \textstyle\sum_{n,t} p_t \cdot dl_{n,t} - \\ \textstyle\sum_{n,t} C_t \cdot dl_{n,t} + \sum_{n,t} S(Dl, dl) - \theta \cdot T \cdot m \end{aligned} \tag{1}$$

$$C_t \le p_t \le \overline{P},\ \forall t \tag{2}$$

$$m \ge \textstyle\sum_n dl_{n,t},\ \forall t \tag{3}$$

The constraints for the DSO optimization are the price range in Eq.(2) and the peak load calculation in Eq.(3).

At the lower level, each LA also tries to maximize its own utility, which consists of its consumption satisfaction and the electricity bill payment in Eq.(4). The resulted load profile is the summation of the thermal load hr and the non-thermal load dr in Eq.(5). Eq.(6) defines the range for the non-thermal load in each time step, and Eq.(7) defines its overall shifting flexibility for the considered decision period. Eq.(8) defines the range for thermal load. The virtual battery constraints in Eq.(9)-(11) are derived based on the building thermal characteristics and are used to guarantee a pre-defined temperature band of each aggregatred building. The difference between the actual power consumed hr by a thermal appliance and its nominal thermal load Dh determines whether the virtual battery is being charged or discharged. ϵ is the virtual battery dissipation rate, which depends on the properties of the thermal load (e.g., insulation characteristics) and can be determined empirically. More details on the virtual battery development can be found in [10]. Eq.(12) ensures that the virtual battery level at the end of the day equals to its initial level.

$$LAs: \max U_n = \textstyle\sum_t S(Dl, dl) - \sum_t p_t \cdot dl_{n,t} \tag{4}$$

$$dl_{n,t} = hr_{n,t} + dr_{n,t} :\ \lambda^{c3}_{n,t} \tag{5}$$

$$\underline{L}_{n,t} \le dr_{n,t} \le \overline{L}_{n,t} :\ \underline{\lambda}^{c4}_{n,t}, \overline{\lambda}^{c4}_{n,t} \tag{6}$$

$$0.9 \cdot \textstyle\sum_t Dd_{n,t} \le \sum_t dr_{n,t} \le 1.1 \cdot \sum_t Dd_{n,t} :\ \underline{\lambda}^{c5}_{n,t}, \overline{\lambda}^{c5}_{n,t} \tag{7}$$

$$\underline{H}_{n,t} \le hr_{n,t} \le \overline{H}_{n,t} :\ \underline{\lambda}^{c6}_{n,t}, \overline{\lambda}^{c6}_{n,t} \tag{8}$$

$$\underline{B}_{n,t} \le b_{n,t} \le \overline{B}_{n,t} :\ \underline{\lambda}^{c7}_{n,t}, \overline{\lambda}^{c7}_{n,t} \tag{9}$$

$$b_{n,t} = \epsilon \cdot (BI_n + hr_{n,t} - Dh_{n,t}) :\ \lambda^{c8}_{n,t=1} \tag{10}$$

$$b_{n,t} = \epsilon \cdot (b_{n,t-1} + hr_{n,t} - Dh_{n,t}) :\ \lambda^{c8}_{n,t\ge 2} \tag{11}$$

$$b_{n,t=T} = BI_n :\ \lambda^{c9}_{n} \tag{12}$$

The consumption satisfaction function $S(Dl, dl)$ is defined as $S(Dl, dl) = Dl_{n,t} \cdot w_{n,t} \cdot f(\frac{dl_{n,t}}{Dl_{n,t}})$ [12] [13] [11]. The $f(x) = x^\alpha$ curve is shown in Fig. 1. Note that $Dl_{n,t} = Dh_{n,t} + Dd_{n,t}$ is the total nominal load; w is a user defined parameter; and α represents the sensitivity of demand shifting.

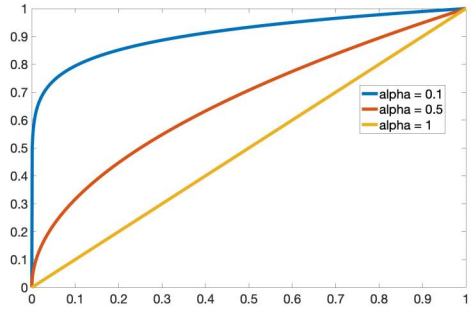

Fig. 1: The $f(x)$ value (y-axis) for different α (x-axis: $\frac{dl}{Dl}$)

To reduce the computational burden and guarantee optimality, the satisfaction function S is linearized into two linear segments at intersection point x_0 where $f'(x_0) = 1$, thus $x_0 = \left(\frac{1}{\alpha}\right)^{\frac{1}{\alpha-1}}$. Since α is also a step dependent parameter, x_0 is different for each time step. Hence, the first linear segment passes through the two points (0, 0) and (x_0, x_0^α), and the second linear segment goes through the two points (x_0, x_0^α) and (1, 1). Thus, the following two satisfaction function constraints need to be added to the lower level model. The lower level model for LAs in the DR game becomes Eq.(4)-(14), where the dual variable of each constraint is presented following a colon.

$$S_{n,t} \le w_{n,t} \cdot x_0^{\alpha_{n,t}-1} \cdot dl_{n,t} :\ \lambda^{c1}_{n,t} \tag{13}$$

$$\begin{aligned} S_{n,t} \le w_{n,t} \cdot dl_{n,t} \cdot \frac{1 - x_0^{\alpha_{n,t}}}{1 - x_0} + \\ w_{n,t} \cdot Dl_{n,t} \cdot \frac{x_0^{\alpha_{n,t}} - x_0}{1 - x_0} :\ \lambda^{c2}_{n,t} \end{aligned} \tag{14}$$

The developed bilevel model in this section is a deterministic model, which corresponds to the risk-neural strategy for the DSO. In the next section, a robust bilevel optimization model is derived based on this deterministic model to cope with the parameter uncertainties.

III. Robust Optimization Model

A. Bilevel robust model

In this section, the robust decision is made from the perspective of the DSO. To consider the related risk of the forecasted parameters $\widetilde{C}_t, \widetilde{Dh}_{n,t}, \widetilde{Dd}_{n,t}$, a new variable set $\Delta = \{\Delta C_t, \Delta Dh_{n,t}, \Delta Dd_{n,t}\}$ is introduced to represent the deviation of the forecasted parameters. The robust factors $\gamma_c, \gamma_h, \gamma_d$ are defined by the decision makers to evaluate the

length of the uncertain gap around the forecasted parameters. Since robust optimization stands at the risk-averse view point, the worst case of uncertainties occurrence in the allowable uncertain range is evaluated [14]. The robust bilevel optimization model for DSO is formulated based on Eq.(1)-(3) as:

$$DSO: \max_{p,dl} \min_{\Delta} U_o = \sum_{n,t} p_t \cdot dl_{n,t} - \sum_{n,t} (\widetilde{C}_t + \Delta C_t) \cdot dl_{n,t} + \sum_{n,t} S(\widetilde{Dl}, dl) - \theta \cdot T \cdot m \tag{15}$$

$$\widetilde{C}_t + \Delta C_t \le p_t \le \overline{P}, \ \forall t \tag{16}$$

$$m \ge \sum_n dl_{n,t}, \ \forall t \tag{17}$$

$$-\gamma_c \cdot \widetilde{C}_t \le \Delta C_t \le \gamma_c \cdot \widetilde{C}_t, \ \forall t \tag{18}$$

$$-\gamma_h \cdot \widetilde{Dh}_{n,t} \le \Delta Dh_{n,t} \le \gamma_h \cdot \widetilde{Dh}_{n,t}, \ \forall n,t \tag{19}$$

$$-\gamma_d \cdot \widetilde{Dd}_{n,t} \le \Delta Dd_{n,t} \le \gamma_d \cdot \widetilde{Dd}_{n,t}, \ \forall n,t \tag{20}$$

As observed in the robust model for the DSO, its objective is maximized with respect to its main decision variables p, dl and minimized by the uncertain parameter set Δ. The length of the uncertain gap can be adjusted by the robust factors.

Similarly, the constraints Eq.(7), Eq.(10), Eq.(11), Eq.(14) in the lower level model are updated as:

$$0.9 \cdot \sum_t (\widetilde{Dd}_{n,t} + \Delta Dd_{n,t}) \le \sum_t dr_{n,t} \le 1.1 \cdot \sum_t (\widetilde{Dd}_{n,t} + \Delta Dd_{n,t}) \tag{21}$$

$$b_{n,t} = \epsilon \cdot (BI_n + hr_{n,t} - \widetilde{Dh}_{n,t} - \Delta Dh_{n,t}) \tag{22}$$

$$b_{n,t} = \epsilon \cdot (b_{n,t-1} + hr_{n,t} - \widetilde{Dh}_{n,t} - \Delta Dh_{n,t}) \tag{23}$$

$$S_{n,t} \le w_{n,t} \cdot dl_{n,t} \cdot \frac{1 - x_0^{\alpha_{n,t}}}{1 - x_0} + w_{n,t} \cdot (Dl_{n,t} + \Delta Dh_{n,t} + \Delta Dd_{n,t}) \cdot \frac{x_0^{\alpha_{n,t}} - x_0}{1 - x_0} \tag{24}$$

The resulted robust bilevel model now becomes the upper level model Eq.(15)-(20) and the lower level model Eq.(4)-(6), Eq.(8)-(9), Eq.(12)-(13), Eq.(21)-(24).

B. Single level robust model

To be able to solve the problem with commercial solvers, the equivalent single level optimization model needs to be obtained. The process to transform the proposed bilevel robust model into a single level model has two main steps: KKT transformation and prime-dual transformation.

In KKT transformation, since the variables in the upper level are treated as parameters in the lower level model of LAs that is then linear and convex, it can be substituted into the upper level model by its equivalent KKT optimality conditions. This process has been conducted in related works frequently [15] [16], for the sake of conciseness, we avoid repeating it here. In this transformation, the strong duality theorem in Eq.(25)-(27) is used to replace the bilinear term $p_t \cdot dl_{n,t}$ in objective Eq.(15). Assume Λ is the prime variables set in the lower model of LA, then

$$\sum_t S_{n,t} - \sum_t p_t \cdot dl_{n,t} = G(\Lambda) + G(\Delta) \tag{25}$$

$$G(\Lambda) = \sum_t \Big[w_{n,t} \cdot (\widetilde{Dh}_{n,t} + \widetilde{Dd}_{n,t}) \cdot \tfrac{x_0^{\alpha} - x_0}{1 - x_0} \cdot \lambda_{n,t}^{c2} - \underline{L}_{n,t} \cdot \underline{\lambda}_{n,t}^{c4} + \overline{L}_{n,t} \cdot \overline{\lambda}_{n,t}^{c4} - \underline{H}_{n,t} \cdot \underline{\lambda}_{n,t}^{c6} + \overline{H}_{n,t} \cdot \overline{\lambda}_{n,t}^{c6} - \underline{B}_{n,t} \cdot \underline{\lambda}_{n,t}^{c7} + \overline{B}_{n,t} \cdot \overline{\lambda}_{n,t}^{c7} \Big] - \sum_t 0.9 \cdot \underline{\lambda}_n^{c5} \cdot \widetilde{Dd}_{n,t} + \sum_t 1.1 \cdot \overline{\lambda}_n^{c5} \cdot \widetilde{Dd}_{n,t} - \sum_t \epsilon \cdot \lambda_{n,t}^{c8} \cdot \widetilde{Dh}_{n,t} + \epsilon \cdot BI_n \cdot \lambda_{n,t=1}^{c8} + BI_n \cdot \lambda_n^{c9} \tag{26}$$

$$G(\Delta) = \sum_t \Big[w_{n,t} \cdot (\Delta Dh_{n,t} + \Delta Dd_{n,t}) \cdot \tfrac{x_0^{\alpha} - x_0}{1 - x_0} \cdot \lambda_{n,t}^{c2} - \sum_t 0.9 \cdot \underline{\lambda}_n^{c5} \cdot \Delta Dd_{n,t} + \sum_t 1.1 \cdot \overline{\lambda}_n^{c5} \cdot \Delta Dd_{n,t} - \sum_t \epsilon \cdot \lambda_{n,t}^{c8} \cdot \Delta Dh_{n,t} \tag{27}$$

After the KKT transformation and $p_t \cdot dl_{n,t}$ replacement in the upper level, the robust bilevel model becomes a single level max-min optimization. Since the minimization in Eq.(15) is with respect to Δ, the objective of the final single level optimization can be rewritten as in Eq.(28)-(29). Together with other related constraints, the final single level max-min model is given as:

$$DSO: \max z \tag{28}$$

$$2 \cdot \sum_{n,t} S_{n,t} - \sum_n G(\Lambda) - \sum_{n,t} \widetilde{C}_t \cdot dl_{n,t} - \theta \cdot T \cdot m - \min_{\Delta} \Big\{ \sum_n G(\Delta) - \sum_{n,t} \Delta C_t \cdot dl_{n,t} \Big\} \ge z \tag{29}$$

$Eq.(16)-(24), Eq.(5)-(6), Eq.(8)-(9), Eq.(12)-(13),$ KKT conditions of the lower level

In order to unify the problem as a final max optimization, the duality theorem is used to convert the inside min optimization to a max optimization by replacing the original min optimization with its max dual optimization problem. The method is well described in [14] [17]. After applying the above transformation, the final single level mixed integer programming model is obtained. The commercial solver CPLEX is used to solve the final model.

IV. Numerical Experiments

In this section, the developed robust bilevel optimization is demonstrated by several groups of experiments. Five LAs are considered in the case study, and the nominal thermal load Dh of each LA consists of residential & commercial HVACs and water heaters, see Fig. 2. The detailed process to generate the data refers to [10] [18]. The nominal non-thermal load Dd in Fig. 3 is adopted from [19] and mixed based on a commercial building reference load. The marginal cost C_t is the same as in [12]. $\alpha_{n,t}$ is assumed the same for all LAs as shown in Fig. 4.

Based on different robust gap length settings γ ($= \gamma_c = \gamma_d = \gamma_h$) on the uncertainties in Eq.(18)-(20) and the peak

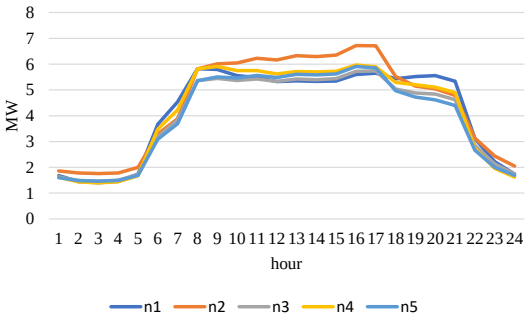

Fig. 2: Nominal thermal load of LAs

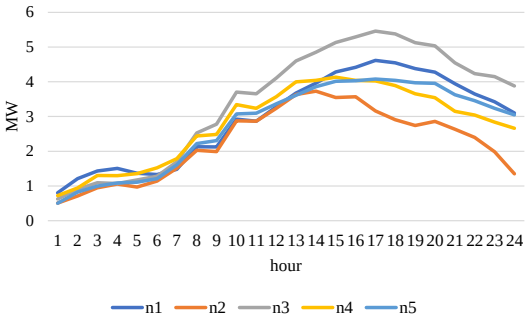

Fig. 3: Nominal non-thermal load of LAs

load penalty θ in Eq.(15), the objective value of the DSO and the resulted peak load from the robust bilevel optimization are illustrated in Fig. 5. As observed, the DSO objective decreases when the penalty θ increases with the same gap level, since the overall satisfaction term and penalty term in the objective function both move against maximization. Furthermore, the DSO objective also drops when the robust gap length increases from 0 to $\pm$ 20%. This is because the robust optimization targets the worst case scenario in the uncertainty range. The peak load has a similar trend, and it is stabilized with max γ despite of the different θ levels due to the flexibility limitation of the load profile.

Take the peak penalty $\theta = 60$ as an example, the resulted electricity prices and load profiles under different uncertainty gap lengths are shown in Fig. 6 and Fig. 7. To optimize against more uncertainties from the wholesale marginal cost and

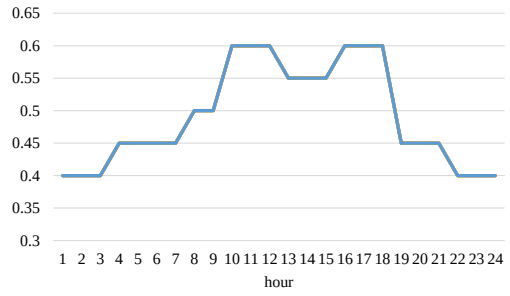

Fig. 4: α preference in satisfaction function

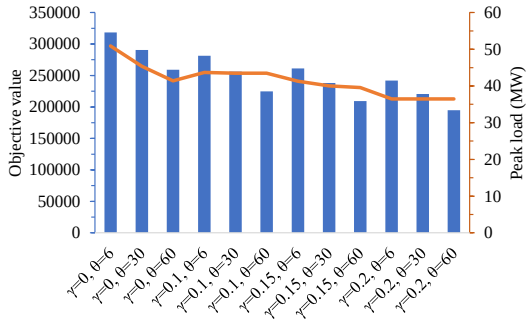

Fig. 5: DSO objective and peak load of the robust optimization under different cases

customers' overall consumption, the DSO tends to increase the prices until the allowable upper bound, especially in the high load range hour 8-21, see the nominal load profile in Fig. 7. The load shifting from peak hours to off-peak hours and peak load reduction can also be observed in Fig. 7.

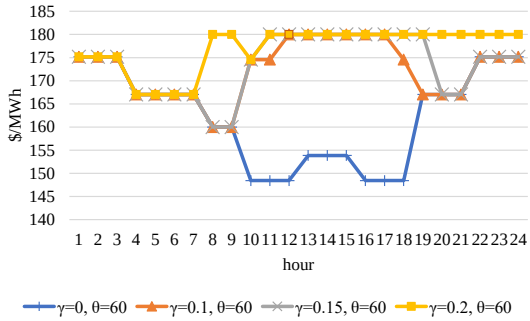

Fig. 6: Price signals of the robust optimization under different cases

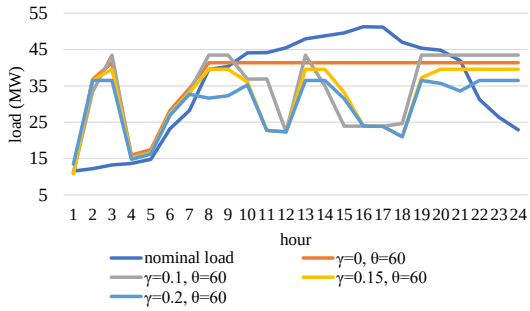

Fig. 7: Resulted load profiles of the robust optimization under different cases

To illustrate the impact of considering uncertainty in the studied problem, after-the-fact analysis is conducted to compare the risk neutral strategy and the proposed robust strategy. After-the-fact scenarios are generated by adding $\pm$ 20% random noise to the three considered uncertainty parameters $C_t, Dh_{n,t}, Dd_{n,t}$. 200 scenarios are generated for the analysis. In Fig. 8, the DSO objective from the robust bilevel model is \$194703 which is the guaranteed lower bound with uncertainty gap $\pm$ 20%, and the objective value from the

neutral model without uncertainty ($\gamma = 0$ assume prediction is accurate) is \$259019. However, after the resulted price decisions from the robust and neutral models are fixed and used to solve the lower level models (Eq.(4)-(12)) over the 200 scenarios, the expected DSO objective value of robust price strategy (\$255185) is higher than the expected objective value of the neutral price strategy (\$231755). These results show the effectiveness of the proposed robust decision approach and thus indicate the importance of modeling uncertainties for risk aversion decision making. The comparison also shows the advantage of robust optimization in guaranteeing a specific level of objective value at certain uncertainty levels.

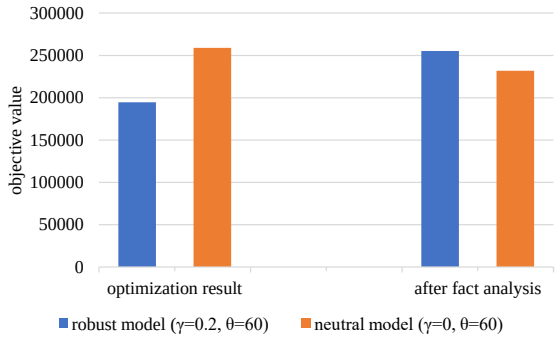

Fig. 8: DSO objectives of robust and neutral strategies in after-the-fact analysis

V. Conclusion

The electricity pricing problem of a DSO is presented in this work with the consideration of DR from LAs and modeled as a bilevel problem. The uncertainties on LAs' energy consumption and the electricity marginal cost are dealt with using a robust optimization with the attitude of risk-averse. Based on the KKT optimality conditions, the lower level model is substituted into the upper level model, and dual transformation is used to convert the nested max-min objective of the DSO into a single level maximization form. The experimental results have shown that the DSO tends to raise the price when the risk of demand uncertainty is higher. Large-scale experiments will be explored in future work with a large number of load aggregators, and possible distributed solution methods will be investigated. Moreover, the robustness of the price strategy from the proposed robust bilevel model is tested against random after-the-fact scenarios and compared to the risk-neutral model. Although the risk-neutral strategy has higher objective value than the robust optimization (worst case), the robust strategy has higher expected objective value than the risk-neutral strategy by taking the actual prediction errors into account, and thus it is more immune to the related risk of predictions.

Acknowledgment

This study was supported by the US Department of Energy (DOE), Office of Energy Efficiency and Renewable Energy, Building Technologies Office under contract DE-AC05-00OR22725.

References

[1] Smart Energy Demand Coalition, "Demand response at the DSO level," https://smarten.eu/demand-response-at-the-dso-level-2/, 2021, accessed Oct. 14, 2021.

[2] International Energy Agency, "Demand response potential in sustainable development scenario, 2018-2040," https://www.iea.org/reports/demand-response, 2021, accessed Oct. 14, 2021.

[3] S. Fan, Q. Ai, and L. Piao, "Bargaining-based cooperative energy trading for distribution company and demand response," *Applied Energy*, vol. 226, pp. 469–482, 2018.

[4] M. Yu and S. H. Hong, "Incentive-based demand response considering hierarchical electricity market: A Stackelberg game approach," *Applied Energy*, vol. 203, pp. 267–279, 2017.

[5] S. Haghifam, M. Dadashi, K. Zare, and H. Seyedi, "Optimal operation of smart distribution networks in the presence of demand response aggregators and microgrid owners: A multi follower bi-level approach," *Sustainable Cities and Society*, vol. 55, p. 102033, 2020.

[6] B. Park, Y. Chen, M. Olama, T. Kuruganti, J. Dong, X. Wang, and F. Li, "Optimal demand response incorporating distribution LMP with PV generation uncertainty," *IEEE Transactions on Power Systems*, pp. 1–1, 2021.

[7] Q. Jia, S. Chen, Z. Yan, and Y. Li, "Optimal incentive strategy in cloud-edge integrated demand response framework for residential air conditioning loads," *IEEE Transactions on Cloud Computing*, pp. 1–1, 2021.

[8] S. Talari, M. Shafie-khah, F. Wang, J. Aghaei, and J. P. S. Catalão, "Optimal scheduling of demand response in pre-emptive markets based on stochastic bilevel programming method," *IEEE Transactions on Industrial Electronics*, vol. 66, no. 2, pp. 1453–1464, 2019.

[9] H. Rashidizadeh-Kermani, M. Vahedipour-Dahraie, M. Shafie-khah, and J. P. Catalão, "Stochastic programming model for scheduling demand response aggregators considering uncertain market prices and demands," *International Journal of Electrical Power & Energy Systems*, vol. 113, pp. 528–538, 2019.

[10] K. Amasyali, Y. Chen, B. Telsang, M. Olama, and S. M. Djouadi, "Hierarchical model-free transactional control of building loads to support grid services," *IEEE Access*, vol. 8, pp. 219 367–219 377, 2020.

[11] Y. Chen, K. Amasyali, B. Park, M. Olama, B. Telsang, and S. Djouadi, "Stochastic pricing game for aggregated demand response considering comfort level," in *Proc. of the 53rd North American Power Symposium (NAPS)*, 2021.

[12] P. Yang, G. Tang, and A. Nehorai, "A game-theoretic approach for optimal time-of-use electricity pricing," *IEEE Transactions on Power Systems*, vol. 28, no. 2, pp. 884–892, 2013.

[13] Y. Chen, M. Olama, X. Kou, K. Amasyali, J. Dong, and Y. Xue, "Distributed solution approach for a Stackelberg pricing game of aggregated demand response," in *Proc. of the IEEE Power Energy Society General Meeting (PESGM)*, 2020, pp. 1–5.

[14] M. Kazemi, H. Zareipour, M. Ehsan, and W. D. Rosehart, "A robust linear approach for offering strategy of a hybrid electric energy company," *IEEE Transactions on Power Systems*, vol. 32, no. 3, pp. 1949–1959, 2017.

[15] Y. Chen, X. Kou, M. Olama, H. Zandi, C. Liu, S. Kassaee, B. T. Smith, A. Abu-Heiba, and A. M. Momen, "Bi-Level Optimization for Electricity Transaction in Smart Community With Modular Pump Hydro Storage," in *Proc. of the ASME 2020 International Design Engineering Technical Conferences and Computers and Information in Engineering Conference*. ASME, Aug. 2020, p. V006T06A016. [Online]. Available: https://doi.org/10.1115/DETC2020-22368

[16] Y. Chen, B. Park, X. Kou, M. Hu, J. Dong, F. Li, K. Amasyali, and M. Olama, "A comparison study on trading behavior and profit distribution in local energy transaction games," *Applied Energy*, vol. 280, p. 115941, 2020.

[17] M. Kazemi, H. Zareipour, N. Amjady, W. D. Rosehart, and M. Ehsan, "Operation scheduling of battery storage systems in joint energy and ancillary services markets," *IEEE Transactions on Sustainable Energy*, vol. 8, no. 4, pp. 1726–1735, 2017.

[18] B. Telsang, K. Amasyali, Y. Chen, M. Olama, and S. Djouadi, "Power allocation by load aggregator with heterogeneous loads using weighted projection," *Energy and Buildings*, vol. 244, p. 110955, 2021.

[19] Y. Chen and M. Hu, "Balancing collective and individual interests in transactive energy management of interconnected micro-grid clusters," *Energy*, vol. 109, pp. 1075–1085, 2016.